


 Cite this: *RSC Adv.*, 2021, 11, 10935

# One-pot conversion of dihydroxyacetone into ethyl lactate by Zr-based catalysts

 Junjun Shi,<sup>ID</sup>\*<sup>a</sup> Fukun Li,<sup>\*bc</sup> Jie Zhang,<sup>b</sup> Ning Li,<sup>b</sup> Xingmin Wang,<sup>b</sup> Xianming Zhang<sup>c</sup> and Yunqi Liu<sup>cd</sup>

Efficient strategies for producing bio-based reagents from sustainable biomass are highly attractive for cost-effective sustainable manufacturing. In this study, a series of eco-friendly Zr-based catalysts (basic zirconium carbonate, zirconium dioxide and zirconium hydroxide) were investigated for the efficient conversion of dihydroxyacetone to ethyl lactate in a one-pot system, in which basic zirconium carbonate exhibited the best performance with 100% dihydroxyacetone conversion and 85.3% EL (ethyl lactate) yield at 140 °C, 4.0 h and 1.0 MPa N<sub>2</sub>. The improved activity of basic zirconium carbonate could be attributed to the synergistic effect among acid and base active sites. Furthermore, this low-cost catalyst shows improved thermochemical stability and recyclability under optimal conditions, where no significant decrease in activity was observed after three runs. This catalytic process could be identified as a promising alternative to produce ethyl lactate from renewable biomass and its derivatives.

 Received 29th January 2021  
 Accepted 8th March 2021

DOI: 10.1039/d1ra00775k

[rsc.li/rsc-advances](https://rsc.li/rsc-advances)

## 1. Introduction

The ever-increasing environmental pollution and energy crisis, caused by the overuse of petroleum resources, urge people to explore and utilize renewable resources. Lignocellulosic biomass, the largest sustainable carbon resource, is recognized as the most promising alternative for producing bio-fuels and bio-based platform chemicals such as levulinic acid, 5-hydroxymethyl furfural, formic acid and ethyl lactate (EL).<sup>1–3</sup> Among them, EL obtained from biomass refinery has attracted growing interest due to its wide application. For example, EL could be applied in food additives, pharmaceuticals, and cosmetics for its low toxicity. Moreover, it can also be employed as a green precursor for the synthesis of other value-added chemicals.<sup>4,5</sup>

Currently, EL is produced predominantly *via* esterification of lactic acid and ethanol catalyzed by H<sub>2</sub>SO<sub>4</sub> (ref. 6) and lipase.<sup>7</sup> However, a number of disadvantages in this procedure should be noted, such as the corrosion of reactor arising from strong mineral acids and the catalyst recycling. Additionally, the precursor, lactic acid, is generally produced *via* fermentation of

biomass, which suffers from low productivity along with tedious post-processing. Therefore, new chemo-catalytic processes from raw biomass and its derivatives directly are intensively required.

Many studies have reported that heterogeneous solid basic catalysts can break down C–C bond in sugars and form alkyl lactates (ALs). For example, a 29.45% yield of methyl lactate (ML) was achieved from glucose under 200 °C in 20 h when MgO was used.<sup>8</sup> Lu *et al.*<sup>9</sup> reported Mg-MOF-74 was an efficient catalyst for converting sucrose to ML with a yield of 47% at 220 °C in 6.0 h. On the other hand, Hayashi *et al.*<sup>10</sup> first reported that Lewis acid salts such as SnCl<sub>2</sub> and SnCl<sub>4</sub> exhibited impressively catalytic activity for the production of ALs in different alcohols. Meanwhile, Holm *et al.*<sup>11</sup> found that Sn-beta zeolite which contained Lewis acid sites could produce ML from mono- and disaccharides. Inspired by these findings, numerous Lewis acid-containing solid materials have been synthesized and used for the preparation of ALs, such as Sn-MCM-41,<sup>12</sup> Sn-MWW,<sup>13</sup> Sn-Mont,<sup>14</sup> SnPO,<sup>15,16</sup> ZrO<sub>2</sub>-TiO<sub>2</sub>,<sup>17</sup> Zr-SBA-15,<sup>18</sup> ZIFs,<sup>19</sup> montmorillonite-supported Pt(II) diphosphane complex<sup>20</sup> and NiO.<sup>21,22</sup> The reported catalysts containing single Lewis acid or base site are responsible for the efficient conversion of dihydroxyacetone (DHA) to lactic acid and its esters.<sup>23</sup> However, the reported catalysts still face a challenge for industrial application due to the complex catalyst preparation procedures or harsh reaction conditions. And little attention was focused on the synergistic effect among acid and base site on a single catalyst.

Zirconium materials possesses important properties: acidity and basicity as well as reducing and oxidizing abilities.<sup>24</sup> Zr-based catalysts, such as ZrO<sub>2</sub>,<sup>25</sup> Zr-containing zeolites,<sup>26</sup> and Zr(OH)<sub>4</sub> (ref. 27) were used for the conversion of biomass. In this study, a one-pot process with Zr-based catalysts possessing

<sup>a</sup>School of Environmental and Chemical Engineering, Foshan University, Foshan 528000, China. E-mail: junjunshi@fosu.edu.cn

<sup>b</sup>Chongqing Engineering Research Center for Processing, Storage and Transportation of Characterized Agro-Products, College of Environment and Resources, Chongqing Technology and Business University, Chongqing 400067, China. E-mail: lfkok@ctbu.edu.cn

<sup>c</sup>Chongqing Key Laboratory of Catalysis & Environmental New Materials, Engineering Research Center for Waste Oil Recovery Technology and Equipment of Ministry of Education, Chongqing Technology and Business University, Chongqing 400067, China

<sup>d</sup>State Key Laboratory of Heavy Oil Processing, China University of Petroleum (East China), Qingdao 266580, China



both Lewis acid and base site for converting DHA to EL under mild conditions was established (Scheme 1). Type of Zr-based catalysts and the impact of various parameters such as catalyst dosage, alcohol choice, reaction temperature and time were also evaluated. In the process proposed here, a remarkable synergistic effect exhibited among Lewis acid and base sites on Zr-based catalyst, giving 100% DHA conversion and 85.3% EL yield. Furthermore, the Zr-based catalyst showed high thermochemical stability and acceptable recyclability.

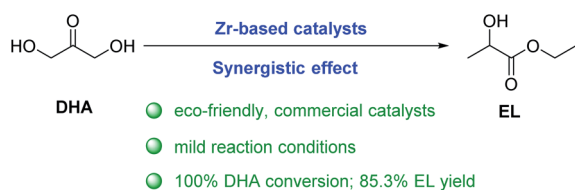
## 2. Materials and methods

### 2.1 Materials

Zr-based catalysts were obtained from Aladdin (Shanghai, China). Naphthalene, DHA, ML, EL, propyl lactate (PL), and butyl lactate (BL) were supplied from TCI Development Co. Ltd (Shanghai, China). Other chemical agents were purchased by Kelong Chemical Factory Co. Ltd (Chengdu, China).  $Zr(CO_3)_2$  was prepared in laboratory by heating basic zirconium carbonate at a temperature of 400 °C for 4.0 h under static air.

### 2.2 Material characterization

The microstructure of materials was investigated by scanning electron microscopy (Bruker, Multimode 8, Germany) at an accelerating voltage of 5.0 kV. Fourier Transform Infrared Spectroscopy (FT-IR) of samples were analyzed by IRPrestige-21 spectrometer (Shimadzu, Japan) using KBr pellets in the range from 400 to 4000  $cm^{-1}$ . X-ray diffraction (XRD) patterns were undertaken on a LabX XRD 6100 diffractometer (Shimadzu, Japan) (Cu  $K\alpha$ -radiation,  $\lambda = 1.5406 \text{ \AA}$ , 40 kV, 40 mA,  $2\theta = 5\text{--}90^\circ$ ) with a scan rate of  $3^\circ \text{ min}^{-1}$ .  $NH_3$  and  $CO_2$  temperature programmed desorption ( $NH_3$ -TPD and  $CO_2$ -TPD) were recorded by a BELCAT II instrument with a thermal conductivity detector (BEL Japan). Each material was heated at 120 °C for 3.0 h under 20  $mL \text{ min}^{-1}$ . He for removing of water and any other physically absorbed gas and then cooled to 100 °C. Subsequently, 20  $mL \text{ min}^{-1}$  5%  $NH_3$  or  $CO_2$  was absorbed for 1.0 h, following by purging with 20  $mL \text{ min}^{-1}$ . He to remove the physically absorbed  $NH_3$  or  $CO_2$  for other 1.0 h. The resulting data was obtained from 100 °C to 470 °C at a rate of  $10^\circ \text{ C min}^{-1}$ .  $N_2$  adsorption-desorption isotherms were obtained by a Micromeritics' ASAP 2020 HD88 Analyzer at  $-196.15^\circ \text{ C}$  before the materials were dehydrated at 100 °C for 24 h under vacuum. Thermogravimetric analysis (TGA) was measured by a STA 449 F3 instrument (Netzsch, Germany). The materials were heated at 80 °C for 6.0 h under vacuum prior to analysis. The curves were



Scheme 1 Conversion of DHA to EL by Zr-based catalysts.

recorded from 40 °C to 850 °C with a heating rate of  $10^\circ \text{ C min}^{-1}$  under a 20  $mL \text{ min}^{-1}$  air.

### 2.3 DHA conversion to EL

The DHA conversion to EL was performed in a 30 mL Teflon-lined stainless-steel autoclave. In a typical experiment, 1.0 mmol DHA, 0.10 g Zr-based catalyst and 10 mL ethanol were loaded into the reactor and exchanged with  $N_2$  for three times and then maintained with a pressure of 1.0 MPa. Subsequently, the reactor was placed into an oil-bath maintained at 140 °C for 4.0 h. After that, the reactor was cooled down to room temperature and the catalyst was recovered by centrifugation and washed with 2 mL ethanol for three times. The recovered catalyst was dried at 60 °C for 6.0 h and used for circulation experiments.

Qualitative analysis of products was carried out on gas chromatography-mass spectrometer apparatus (Shimadzu, GCMS-QP2020) with SH-Rxi-5Sil MS column (30 m, 0.25 mm  $\times$  0.25  $\mu\text{m}$ ). The conversion of DHA was carried out on a high-performance liquid chromatography instrument (Agilent 1200 HPLC) equipped with a refractive index detector (RID) and an HPX-87H column (300 mm  $\times$  7.8 mm, 5  $\mu\text{m}$ ) using the standard curve method. And the products were conducted on a Shimadzu GC-2010 Plus equipped with a flame ionization detector (FID) and RTX®-5 column (30 m, 0.25 mm  $\times$  0.25  $\mu\text{m}$ ) based on the internal standard method (naphthalene as the internal standard). DHA conversion ( $C_{DHA}$ ) and EL yield ( $Y_{EL}$ ) were expressed as following the eqn (1) and (2):

$$C_{DHA}(\text{mol}\%) = \left(1 - \frac{M_{F2}}{M_{F1}}\right) \times 100\% \quad (1)$$

$$Y_{EL}(\text{mol}\%) = \frac{M_{EL}}{M_{F1}} \times 100\% \quad (2)$$

where  $M_{F1}$  and  $M_{F2}$  stand for the mole of DHA before and after reaction, respectively, and  $M_{EL}$  stands for the mole of EL quantified by GC.

## 3. Results and discussion

### 3.1 Catalyst characterization

XRD pattern of basic zirconium carbonate indicates that this material is amorphous in nature with no obvious diffraction peaks. Small size particles without uniform structure could be observed in SEM images, which is well accorded with the XRD pattern (Fig. 1a). Furthermore,  $N_2$  physisorption profile demonstrates that basic zirconium carbonate possesses a typical type IV isotherm with a H3-type hysteresis loop and a broad distribution of pore sizes (Fig. 1b). In the solid FT-IR spectrogram (Fig. 1c), the peaks between 3220 and 3680  $cm^{-1}$  can be assigned to the  $-OH$  stretching on the catalyst surface or absorbed trace water.<sup>28</sup> Absorption at 2350  $cm^{-1}$  is asymmetric stretching of  $CO_2$ . The two signals at 1515 and 1367  $cm^{-1}$  and the single peak located at 1081  $cm^{-1}$  are attributed to the asymmetric stretching and symmetric stretching of  $CO_3^{2-}$ , respectively.<sup>29</sup> The peak detected at 836  $cm^{-1}$  is considered as the stretching of  $Zr-O$ .<sup>30</sup>

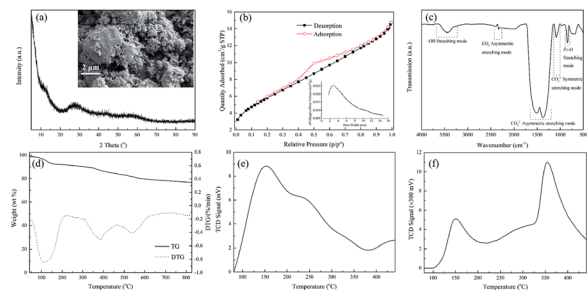


Fig. 1 Basic zirconium carbonate characterization: (a) SEM image and XRD pattern, (b)  $N_2$  physisorption profile, (c) FT-IR profile, (d) TG-DTG curve, (e)  $NH_3$ -TPD profile and (f)  $CO_2$ -TPD profile.

Additionally, the thermal behavior of Zr-based catalyst (Fig. 1d) was also analyzed by TG-DTG. It shows that basic zirconium carbonate has three degradation peaks. Between 40 and 227 °C, the weight loss (8.5 wt%) can be assigned to the removal of adsorbed and structural water. The second one (227–463 °C) exhibits a 7.4 wt% weight loss, which can be explained by the dehydration of hydroxyl groups upon the basic zirconium carbonate.<sup>29</sup> Further increased to 550 °C, 5.2 wt% weight loss can be observed due to the decomposition of  $CO_3^{2-}$ .<sup>28</sup> The above results clearly suggest that the catalyst has high thermal stability over a broad temperature, which can be applied in biomass refinery.  $NH_3$ -TPD curve shows basic zirconium carbonate can be classified as weak and moderate acid sites (Fig. 1e). Meanwhile, we can also observe the coexistence of weak, moderate, and strong base sites based on the desorption temperature, respectively (Fig. 1f), demonstrating that surface of basic zirconium carbonate exhibits both acid and base characteristics, which is important to establish the impressive activity and selectivity of EL in this catalyst system.

### 3.2 Catalytic performance of Zr-based materials

The catalytic activities of various Zr-based catalysts were investigated for converting DHA into EL at 140 °C for 4.0 h. The result shows that the conversion of DHA to EL is insignificant without any catalyst (only 5.1%, Table 1, entry 1). However, when various Zr-based catalysts were employed, a remarkable increase of conversion and EL yield could be observed. For example, basic zirconium carbonate showed the best performance, giving 100% DHA conversion with 85.3% EL yield (Table 1, entry 2). Whereas, the yield of EL decreased to 57.6% with  $Zr(OH)_4$  (Table 1, entry 3). It is worth noting that clear difference was observed in product distribution using  $ZrO_2$  as the catalyst (Table 1, entry 4), where the major product was ethyl acetal of pyruvic aldehyde (EAPA, 38.9% yield).

In general, piperidine and benzoic acid, as the deactivators of acid/base sites upon the surface of catalyst, were employed to explore the role of acid and base sites during the reaction. As shown in Table 1, it can be seen that a notable decrease of EL yield was achieved in the presence of either probe molecules. For example, DHA conversion decreased from 100% to 70.4% and 63.2%, accompanying with EL yield decreasing from 85.3% to 55.1% and 50.7% with 1.0 mmol piperidine or benzoic acid,

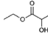
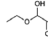
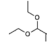
respectively (Table 1, entries 2, 5 and 6), demonstrating that single Lewis acid or base site shows lower active.<sup>12,31</sup> Besides, selectivity for EL production slightly decreased from 85.3% to 78.2% and 80.3% in the presence of piperidine and benzoic acid. These results suggested that the synergistic effect among acid and base sites of catalyst plays a key role in the formation of EL.

To further understand the effect of active sites on the complex structure of basic zirconium carbonate ( $Zr-OH$ ,  $Zr=O$  and  $Zr-CO_3$ ), a series of comparing catalysts ( $NaOH$  for  $-OH$ ,  $Zr(OH)_4$  for  $Zr-OH$ ,  $ZrO_2$  for  $Zr=O$ ,  $Na_2CO_3$  for  $-CO_3$ , and  $Zr(CO_3)_2$  for  $Zr-CO_3$ ) were employed. Only 40.3% EL was obtained with  $NaOH$  (Table 1, entry 7), lower than that from  $Zr(OH)_4$  catalyst of 57.6% (Table 1, entry 3), which can be attributed to the formation of humins from glyceraldehyde *via* the isomerization of DHA in the presence of strong base.<sup>32</sup> Meanwhile, as shown in Table 1, it is also noticed that either  $Zr(CO_3)_2$  or  $Na_2CO_3$  exhibited lower catalytic activity on EL production but higher EAPA yield (Table 1, entries 8 and 9). For example, EL yield obtained from  $Zr(CO_3)_2$  was 12.7%, which was much lower than  $Zr(OH)_4$  of 57.6%. However, EAPA yield from  $Zr(CO_3)_2$  (43.1%) was much higher than that from  $Zr(OH)_4$  (only 0.8%). It is indicated that  $Zr-OH$  was the active site for EL in our process, which is well consistent with the previous study that  $M-OH$  is responsible for the conversion EAPA to EL.<sup>33</sup> In addition, the EL yield decreased from 85.3% to 68.3% under 1.0 MPa  $O_2$  (Table 1, entries 2 and 10), which may be attributed to the oxidation of carbonyl (aldehyde) group by superoxide radical anions according to Lin's work.<sup>34</sup> Furthermore, 90.8% DHA conversion and 78.9% EL yield could still be achieved after three runs (Table 1, entry 11), demonstrating that the basic zirconium carbonate catalyst has good recyclability.

### 3.3 The effect of various reaction parameters

The effect of reaction temperature and time on process efficiency of EL production is presented in Fig. 2a and b, which shows that this process is highly temperature-dependent. For example, EL yield remarkably increased from 45.1% to 82.9% accompanying with DHA conversion improved from 73.3% to 97.8% when the temperature was rose from 120 to 150 °C at 1.0 h. Both the DHA conversion and EL yield could also be enhanced by the extending reaction time. For example, 100% DHA conversion and 83.1% EL yield can be obtained by extending the reaction time to 7.0 h. Furthermore, the yield of DEPAP, the only by-product detected, was decreased from 20.2% to 4.5% when the temperature rose from 120 to 150 °C. This indicates that higher temperature facilitates the conversion of EAPA to EL but lower temperature favors conversion EAPA to DEAPA, which is well accordance with the previously reported works.<sup>35,36</sup> Besides, the DEAPA yield decreased with the increase of reaction time and temperature, which could be explained by the conversion of DEAPA to EAPA and further to EL.<sup>17</sup> For example, under 120 °C and 5.0 h, 100% DHA conversion and 75.9% EL yield were obtained, and the EL yield increased to 83.1% with extending reaction time to 7.0 h. Thus,

Table 1 Catalytic activity tests of Zr-based catalysts<sup>a</sup>

| Entry           | Catalyst   | Conversion (%) | Yield <sup>b</sup> (%)  |  |   | Selectivity (%) |
|-----------------|--|----------------|---|--|---|-----------------|
|                 |  |                |  |  |  |                 |
| 1               | Blank  | 5.1 ± 0.9      | — <sup>c</sup>  | —  | —   | —               |
| 2               | (ZrO) <sub>2</sub> CO <sub>3</sub> (OH) <sub>2</sub> | 100            | 85.3 ± 1.2  | —  | 1.3 ± 1.1   | 85.3 ± 1.4      |
| 3               | Zr(OH) <sub>4</sub>                                  | 100            | 57.6 ± 1.8  | 0.8 ± 0.3  | 2.8 ± 0.5   | 57.6 ± 1.3      |
| 4               | ZrO <sub>2</sub>                                     | 76.3 ± 1.7     | 8.1 ± 0.9   | 38.9 ± 1.3   | 3.4 ± 0.8   | 10.6 ± 1.0      |
| 5 <sup>d</sup>  | (ZrO) <sub>2</sub> CO <sub>3</sub> (OH) <sub>2</sub> | 70.4 ± 1.4     | 55.1 ± 1.8  | —  | 3.7 ± 1.1   | 78.2 ± 1.4      |
| 6 <sup>e</sup>  | (ZrO) <sub>2</sub> CO <sub>3</sub> (OH) <sub>2</sub> | 63.2 ± 1.3     | 50.7 ± 0.7  | —  | 4.3 ± 1.5   | 80.3 ± 0.9      |
| 7               | NaOH   | 100            | 40.3 ± 1.7  | —  | —   | 40.3 ± 1.6      |
| 8               | Zr(CO <sub>3</sub> ) <sub>2</sub>                    | 81.7 ± 1.9     | 10.4 ± 0.7  | 43.1 ± 2.1   | 4.9 ± 1.1   | 12.7 ± 1.3      |
| 9               | Na <sub>2</sub> CO <sub>3</sub>                      | 37.1 ± 1.8     | 2.7 ± 1.1   | 10.5 ± 1.3   | 3.1 ± 1.0   | 7.3 ± 1.2       |
| 10 <sup>f</sup> | (ZrO) <sub>2</sub> CO <sub>3</sub> (OH) <sub>2</sub> | 100            | 68.3 ± 2.1  | —  | 1.8 ± 0.7   | 68.3 ± 1.8      |
| 11 <sup>g</sup> | (ZrO) <sub>2</sub> CO <sub>3</sub> (OH) <sub>2</sub> | 90.8 ± 1.7     | 78.9 ± 2.0  | —  | 3.3 ± 1.1   | 86.8 ± 1.4      |

<sup>a</sup> Reaction conditions: 1.0 mmol DHA, 0.10 g catalyst, 10 mL ethanol, 140 °C, 4.0 h, 1.0 MPa N<sub>2</sub>. <sup>b</sup> The products listed as following: ethyl lactate (EL), ethyl acetal of pyruvic aldehyde (EAPA), diethyl acetal of pyruvic aldehyde (DEAPA). <sup>c</sup> (—): not detected. <sup>d</sup> Adding with 1.0 mmol piperidine. <sup>e</sup> Adding with 1.0 mmol benzoic acid. <sup>f</sup> 1.0 MPa O<sub>2</sub>. <sup>g</sup> The 3<sup>th</sup> cycle of basic zirconium carbonate.

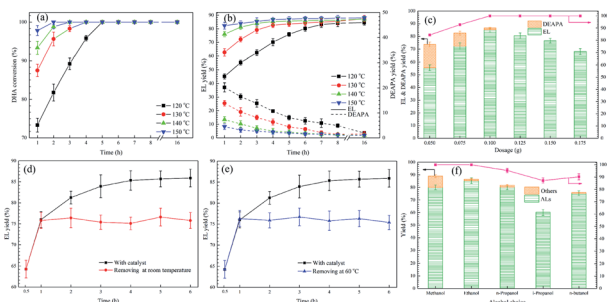


Fig. 2 Effects of various parameters on transformation of DHA to EL over basic zirconium carbonate: (a and b) reaction temperature and time, 1.0 mmol DHA, 0.10 g basic zirconium carbonate, 10 mL ethanol; (c) dosage, 1.0 mmol DHA, 10 mL ethanol, 140 °C, 4.0 h; (d and e) leaching tests, 1.0 mmol DHA, 0.10 g basic zirconium carbonate, 10 mL ethanol, 140 °C; (f) alcohol choice, 1.0 mmol DHA, 0.10 g basic zirconium carbonate, 10 mL alcohol, 140 °C, 4.0 h, others stands for the resulting dialkylacetal of pyruvic aldehyde except in methanol media where 1,1,2,2-tetramethoxypropane is the only detected by-product.

from the above discussion, 140 °C and 4.0 h are required to achieve excellent process efficiency.

Fig. 2c shows that catalyst dosage plays a critical role in the conversion of DHA to EL. A negligible process efficiency was observed without any catalyst (Table 1, entry 1). However, it was significantly improved after adding 0.05 g basic zirconium carbonate, giving 85.3% DHA conversion and 55.5% EL yield (Fig. 2c). The peak value of EL yield (85.3%) was achieved at 0.10 g catalyst. However, a decrease trend of EL yield was obtained when catalyst loading increased to 0.175 g. Hence, 0.10 g of the catalyst would be the optimum amount at 140 °C for 4.0 h.

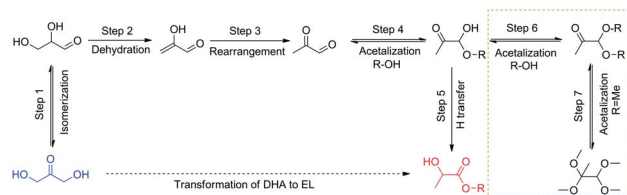
Leaching tests were also conducted to investigate the chemical stability under optimal conditions. As exhibited in

Fig. 2d and e, the EL yield remained approximately constants after removing the catalyst for 1.0 h with both cold (room temperature) and hot (60 °C) filtration. Meanwhile, no zirconium ions were detected in the above filtrates by ICP-AES analysis. These findings demonstrate that the active sites on the surface of the catalyst are stable during the process.

Inspired by the outstanding catalytic performance of basic zirconium carbonate for converting DHA to EL in ethanol, the influence of alcohol choice was further investigated. In Fig. 2f, the process efficiency changed markedly in different alcohols. With methanol, a slight decrease of ML yield (80.1%) was shown compared to that with ethanol (85.3%), which can be attributed to the lowest steric hindrance, resulting in the formation of 1,1,2,2-tetramethoxypropane (8.9%).<sup>14</sup> Further extending the carbon chain of *n*-alcohol, a declined trend of the corresponding alkyl lactates yield was observed, which may be explained by the increasing effect of steric hindrance. For example, only 75.4% BL yield was generated from *n*-butanol. This effect of steric hindrance was more obvious for *i*-propanol, where only 60.2% isopropyl lactate yield was achieved.

### 3.4 Reaction pathway of the DHA conversion

Based on the above discussion and previous reports,<sup>37–43</sup> a probable reaction pathway for transformation of DHA to EL is



Scheme 2 Reaction pathway for conversion of DHA to EL over basic zirconium carbonate.



proposed (Scheme 2). Firstly, the DHA is isomerized to glycer-aldehyde (Step 1).<sup>37</sup> The dehydration and rearrangement reaction catalyzed by both Brønsted and Lewis acids undergoes, giving an important intermediate compound-pyruvic aldehyde (PAL) (Step 2 and 3).<sup>38–40</sup> Then pyruvic aldehyde further converted to hemiacetal through nucleophilic attack on aldehyde carbonyl group with alcohol (Step 4).<sup>39</sup> At last, EL can be achieved by intramolecular H transfer of hemi-ethyl acetal of pyruvic aldehyde, which is solely catalyzed by Lewis acids (Step 5).<sup>41–43</sup> Besides, dialkylacetal of pyruvic aldehyde can be obtained by etherification between alkyl acetal of pyruvic aldehyde and alcohol solvent (Step 6). With methanol, pyruvaldehyde dimethyl acetal can be further converted to 1,1,2,2-tetraethoxypropane due to its low steric hindrance (Step 7).<sup>14</sup> It should be noted that two key intermediate products, namely, 2-hydroxyacrylaldehyde pyruvic aldehyde, and pyruvic aldehyde. However, they are hard to be detected directly due to the high reactivity.<sup>14</sup> Instead, the formation of pyruvic aldehyde could be confirmed by the detected diethyl acetal of pyruvic aldehyde. Therefore, it is suggested that the intramolecular H transfer of hemi-alkyl acetal of pyruvic aldehyde is more likely to be the rate-determining step in this cascade reaction.<sup>10</sup> According previous reports, this rate-limited step involves similar mechanism of Meerwein–Ponndorf–Verley reduction, which is closely related with synergistic effect among the acid and base of the catalyst.<sup>33,44</sup>

## 4. Conclusions

A new eco-friendly strategy for the efficient conversion of DHA to ALs was achieved using basic zirconium carbonate by virtue of its synergistic effect among acid and base sites. At selected condition of 140 °C, 4.0 h and 1.0 MPa N<sub>2</sub>, 100% DHA conversion and 85.3% EL yield was achieved. The basic zirconium carbonate had a high chemical stability and good recyclability with maintaining acceptable catalytic activity after three cycles. Thus, this efficient catalytic system has a promising alternative for EL production from renewable biomass.

## Conflicts of interest

There are no conflicts to declare.

## Acknowledgements

The authors gratefully acknowledge the financial support of the National Natural Science Foundation of China (Grant No. 21808021 and 21808032), the Natural Science Foundation of Guangdong Province (Grant No. 2018A030310351), the Science and Technology Research Program of Chongqing Municipal Education Commission (Grant No. KJQN201800828, KJZD-M201900802 and KJZD-K201800801) and the Startup Foundation of Chongqing Technology and Business University (Grant No. 950318060).

## References

- 1 Z. Cai, J. Long, Y. Li, L. Ye, B. Yin, L. J. France, J. Dong, L. Zheng, H. He, S. Liu, S. C. E. Tsang and X. Li, *Chem*, 2019, **5**, 1.
- 2 J. Y. Kim, H. W. Lee, S. M. Lee, J. Jae and Y. K. Park, *Bioresour. Technol.*, 2019, **279**, 373.
- 3 D. P. Yang, Z. Li, M. Liu, X. Zhang, Y. Chen, H. Xue, E. Ye and R. Luque, *ACS Sustainable Chem. Eng.*, 2019, **7**, 4564.
- 4 S. M. Nikles, M. Piao, A. M. Lane and D. E. Nikles, *Green Chem.*, 2001, **3**, 109.
- 5 W. Zhang, P. Oulego, T. K. Slot, G. Rothenberg and N. R. Shiju, *ChemCatChem*, 2019, **11**, 3381.
- 6 R. A. Troupe and E. DiMilla, *Ind. Eng. Chem. Res.*, 1957, **49**, 847.
- 7 M. Koutinas, C. Yiangou, N. M. Osório, K. Ioannou, A. Canet, F. Valero and S. Ferreira-Dias, *Bioresour. Technol.*, 2018, **247**, 496.
- 8 Z. Liu, W. Li, C. Pan, P. Chen, H. Lou and X. Zheng, *Catal. Commun.*, 2011, **15**, 82.
- 9 X. Lu, L. Wang and X. Lu, *Catal. Commun.*, 2018, **110**, 23.
- 10 Y. Hayashi and Y. Sasaki, *Chem. Commun.*, 2005, **21**, 2716.
- 11 M. S. Holm, S. Saravanamurugan and E. Taarning, *Science*, 2010, **328**, 602.
- 12 F. de Clippel, M. Dusselier, R. Van Rompaey, P. Vanelderden, J. Dijkmans, E. Makshina, L. Giebel, S. Oswald, G. V. Baron, J. F. M. Denayer, P. P. Pescarmona, P. A. Jacobs and B. F. Sels, *J. Am. Chem. Soc.*, 2012, **134**, 10089.
- 13 Y. R. Hu, F. Wang, S. K. Wang, C. Z. Liu and C. Guo, *Bioresour. Technol.*, 2013, **138**, 387.
- 14 J. Wang, Y. Masui and M. Onaka, *Appl. Catal., B*, 2011, **107**, 135.
- 15 X. Wang, F. Liang, C. Huang, Y. Li and B. Chen, *Catal. Sci. Technol.*, 2015, **5**, 4410.
- 16 X. Wang, F. Liang, C. Huang, Y. Li and B. Chen, *Catal. Sci. Technol.*, 2016, **6**, 6551.
- 17 A. M. Mylin, S. I. Levytska, M. E. Sharanda and V. V. Brei, *Catal. Commun.*, 2014, **47**, 36.
- 18 L. Yang, X. Yang, E. Tian, V. Vattipalli, W. Fan and H. Lin, *J. Catal.*, 2016, **333**, 207.
- 19 B. Murillo, B. Zornoza, O. de la Iglesia, C. Téllez and J. Coronas, *J. Catal.*, 2016, **334**, 60.
- 20 W. Oberhauser, C. Evangelisti, S. Caporali, V. Dal Santo, F. Bossola and F. Vizza, *J. Catal.*, 2017, **350**, 133.
- 21 X. Lyu, L. Wang, X. Chen, L. Xu, J. Wang, S. Deng and X. Lu, *Ind. Eng. Chem. Res.*, 2019, **58**, 3659.
- 22 X. Lyu, M. Xu, X. Chen, L. Xu, J. Wang, S. Deng and X. Lu, *Ind. Eng. Chem. Res.*, 2019, **58**, 12451.
- 23 P. Mäki-Arvela, I. L. Simakova, T. Salmi and D. Y. Murzin, *Chem. Rev.*, 2013, **114**, 1909.
- 24 G. Yang, Y. Ke, H. Ren, C. Liu, R. Yang and W. Dong, *Chem. Eng. J.*, 2016, **283**, 759.
- 25 P. Wattanapaphawong, P. Reubroycharoen and A. Yamaguchi, *RSC Adv.*, 2017, **7**, 18561.

- 26 J. Wang, K. Okumura, S. Jaenicke and G.-K. Chuah, *Appl. Catal., A*, 2015, **493**, 112.
- 27 X. Tang, H. Chen, L. Hu, W. Hao, Y. Sun, X. Zeng, L. Lin and S. Liu, *Appl. Catal., B*, 2014, **147**, 827.
- 28 P. A. Son, S. Nishimura and K. Ebitani, *React. Kinet., Mech. Catal.*, 2014, **111**, 183.
- 29 A. Bohre, B. Saha and M. M. Abu-Omar, *ChemSusChem*, 2015, **8**, 4022.
- 30 M. Mahdavi and A. Ghiasi, *Ceram. Int.*, 2016, **42**, 7203.
- 31 S. Yamaguchi, M. Yabushita, M. Kim, J. Hirayama, K. Motokura, A. Fukuoka and K. Nakajima, *ACS Sustainable Chem. Eng.*, 2018, **6**, 8113.
- 32 A. Takagaki, H. Goto, R. Kikuchi and S. T. Oyama, *Appl. Catal., A*, 2019, **570**, 200.
- 33 E. Taarning, S. Saravanamurugan, M. S. Holm, J. Xiong, R. M. West and C. H. Christensen, *ChemSusChem*, 2009, **2**, 625.
- 34 H. Lin, J. Strull, Y. Liu, Z. Karmiol, K. Plank, G. Miller, Z. Guo and L. Yang, *Energy Environ. Sci.*, 2012, **5**, 9773.
- 35 P. Y. Dapsens, B. T. Kusema, C. Mondelli and J. Pérez-Ramírez, *J. Mol. Catal. A: Chem.*, 2014, **388**, 141.
- 36 P. P. Pescarmona, K. P. F. Janssen, C. Delaet, C. Stroobants, K. Houthoofd, A. Philippaerts, C. De Jonghe, J. S. Paul, P. A. Jacobs and B. F. Sels, *Green Chem.*, 2010, **12**, 1083.
- 37 R. S. Assary and L. A. Curtiss, *J. Phys. Chem. A*, 2011, **115**, 8754.
- 38 M. A. Hossain, K. N. Mills, A. M. Molley, M. S. Rahaman, S. Tulaphol, S. B. Lalvani, J. Dong, M. K. Sunkara and N. Sathitsuksanoh, *Appl. Catal., A*, 2021, **611**, 117979.
- 39 A. Feliczak-Guzik, M. Sprynskyy, I. Nowak and B. Buszewski, *Catalysts*, 2018, **8**, 31.
- 40 P. Y. Dapsens, C. Mondelli and J. Pérez-Ramírez, *ChemSusChem*, 2013, **6**, 831.
- 41 L. Cheng, C. Doubleday and R. Breslow, *Proc. Natl. Acad. Sci. U. S. A.*, 2015, **112**, 4218.
- 42 S. Lux and M. Siebenhofer, *Catal. Sci. Technol.*, 2013, **3**, 1380.
- 43 E. Jolimaitre, D. Delcroix, N. Essayem, C. Pinel and M. Besson, *Catal. Sci. Technol.*, 2018, **8**, 1349.
- 44 J. Song, B. Zhou, H. Zhou, L. Wu, Q. Meng, Z. Liu and B. Han, *Angew. Chem., Int. Ed.*, 2015, **54**, 9399.